Cell-free Embryonic Stem Cell Extract-mediated Derivation of Multi-potent Stem Cells from NIH3T3 Fibroblasts for Functional and Anatomical Ischemic Tissue Repair

Johnson Rajasingh[1], Hiromichi Hamada[1], Evelyn Bord[1], Tina Thorne[1], Ilona Goukassian[1], Erin Lambers[1], Prasanna Krishnamurthy[1], Gangjian Qin[1], Karen Schlauch[2], Kenneth M. Rosen[3], Deepali Ahluwalia[1], Yan Zhu[4], Douglas W. Losordo[1], Raj Kishore[1]

[1]Feinberg Cardiovascular Research Institute, Feinberg School of Medicine, Northwestern University, 303 E Chicago Avenue, Chicago IL 60611, [2]Department of Genetics and genomics, Boston University School of Medicine, Boston, MA, [3]Division of Neurology Research, [4]Division of Cardiovascular Research, Caritas St. Elizabeth's Medical Center, Tufts University School of Medicine, Boston, MA 02135

Address correspondence and reprint requests to:

Raj Kishore Ph.D

Feinberg Cardiovascular Research Institute

Feinberg School of Medicine, Northwestern University

303 E Chicago Avenue, Chicago IL 60611

Telephone: 312-503-1651, Fax: 312-503-1655

E.mail: r-kishore@northwestern.edu

The oocyte-independent generation of multipotent stem cells is one of the goals in regenerative medicine. We report that upon exposure to mouse ES cell (ESC) extracts, reversibly permeabilized NIH3T3 cells undergo de-differentiation followed by stimulus-induced re-differentiation into multiple lineage cell types. Genome-wide expression profiling revealed significant differences between NIH3T3 and ESC-extract treated NIH3T3 cells including re-activation of ESC specific transcripts. Epigenetically, ESC extracts induced CpG de-methylation of Oct4 promoter, hyper-acetylation of histones 3 and 4 and decreased lysine 9 (K-9) dimethylation of histone 3. In mouse models of surgically-induced hind limb ischemia (HLI) or acute myocardial infarction (AMI) transplantation of reprogrammed NIH3T3 cells significantly improved post-injury physiological functions and showed antomical evidence of engraftment and trans-differentiation into skeletal muscle, endothelial cell and cardiomyocytes. These data provide evidence for the generation of functional multi-potent stem like cells from terminally differentiated somatic cells without the introduction of trans-genes or ESC fusion.

The available evidence demonstrating improvement in myocardial function following transplantation of autologous bone marrow (BM) derived stem/progenitor cells, both in pre-clinical as well as in available clinical trials, remains a potent force driving discovery and clinical development simultaneously and has provided new hope for patients with debilitating heart diseases[1, 2]. However, certain potential limitations of autologous BM or peripheral blood derived stem/progenitor cells have also been identified. Risk factors for coronary artery disease are reported to be associated with a

reduced number and impaired functional activity of endothelial progenitor cells (EPC) in the peripheral blood of patients[3-6].

De-differentiation of adult somatic cells into multi-potent cells might provide an attractive source of stem cells for regenerative medicine including post-infarct cardiac and other ischemic tissue repair. Recent experimental evidence has revealed that nuclear re-programming of terminally differentiated adult mammalian cells leading to their de-differentiation is possible[7-10]. The best example of somatic cell nuclear re-programming comes from reproductive and therapeutic cloning experiments utilizing somatic nuclear transfer (SNT), wherein transplantation of somatic nuclei into enucleated oocyte cytoplasm can extensively reprogram somatic cell nuclei with new patterns of gene expression, new pathways of cell differentiation and successful generation of embryonic stem cells and birth of cloned animals[11-15]. Therapeutic cloning by SNT for clinical application, though conceptually attractive is yet not practical given the technical difficulties, extremely low efficiency, oocyte-dependence, ethico-legal concerns and prohibitive cost associated with the process. It, therefore, becomes imperative to develop alternative strategies for somatic cell re-programming. One strategy would be to develop oocyte-independent systems, for instance, exposure of somatic cell nuclei to ESC-derived cell-free factors/proteins to drive somatic cell de-differentiation and nuclear re-programming. Indeed, alterations in the fate of one kind of differentiated somatic cells by cell-free extracts from other, leading to the acquirement of donor cell characteristics and functions by recipient cells, has been previously reported[16-22].

In the present study we report that exposure to mouse ESC extracts induces marked epigenetic reprogramming in NIH3T3 fibroblasts including re-activation of ESC specific gene expression. These re-programmed cells possess multi-potent stem cell like characteristics including multi-

lineage differentiation potential and more importantly therapeutic efficacy for improvement in physiological functions and anatomical tissue repair in mouse models of surgically induced hind limb ischemia and acute myocardial infarction.

RESULTS

Exposure of NIH3T3 fibroblasts to mES cell extracts leads to the induction of ESC specific genes

Reversibly permeabilized (by Sreptolysin O) NIH3T3 cells were exposed to either with whole cell extracts from NIH3T3 ('self' as control) or D3 in ATP-regenerating reaction (see Methods). Plasma membranes were sealed by including 2mM calcium chloride in medium and cells were further cultured in D3 maintenance medium (complete DMEM + 10 ng/mL of LIF. NIH3T3 cells treated with the self extracts (hereto referred as 3T3) did not show any morphological changes up to day 10 post-treatment (**Fig. 1A[a]**), whereas NIH3T3 cells treated with D3 extracts (hereto referred as 3T3/D3) showed noticeable changes in cell morphology as early as day 3 post-treatment forming colonies resembling typical ESC morphology by day 10 **(Fig. 1A [b-d])**. Individual colonies were culture expanded and characterized. To determine if the altered morphology of 3T3/D3 cells represents the de-differentiation of NIH3T3 cells, we analyzed the induction of mESC markers in 3T3/D3 and 3T3 cells up to 4 weeks post-treatment, both at the mRNA and protein level. Quantitative mRNA expression of mESC specific transcripts Oct4, Nanog, SSEA1, SCF and c-Kit was induced in 3T3/D3 cells while 3T3 cells did not express measurable mRNA for any of these stem cell markers (**Fig. 1B**). Enhanced mRNA expression of stem cell specific genes was further corroborated by immuno-fluorescence staining for selected proteins Oct4 (**Fig. 1C**), c-Kit and SSEA1 (see **Supplementary Fig. S1B,C** online). Further corroboration of NIH3T3 de-

differentiation was evident by the loss of lamin-A protein expression, a specific marker of somatic cells, in 3T3/D3 cells (**Fig. 1D,E**). Taken together, these data suggest that as an alternative to ESC-somatic cell fusion and somatic nuclear transfer[7, 9, 10], cell-free ESC extracts could provide the necessary regulatory components required to induce somatic nuclear reprogramming and alter the differentiation status of non-embryonic cells. We further confirmed whether the D3 proteins and not the contaminating nucleic acids drive 3T3 de-differentiation. Inactivation of proteins from D3 extracts prior to reaction either by temperature, trypsin or proteinase K digestion failed to induce any mprphological changes or to the activation of Oct4 mRNA (**see Supplementary figure S2 online**), whereas inactivation of either DNA or RNA had no such effect.

D3-extract induced epigenetic changes in NIH3T3 cells involve Oct4 promoter demethylation and Histone 3 modifications.

DNA methylation of CpG residues leading to the silencing of pluripotent embryonic genes, including that of Oct4, is known as an integral step governing differentiation and development. Since our data indicated that D3-extract exposure leads to the induction of Oct4 mRNA and protein expression in 3T3/D3 cells, we performed studies to determine whether D3-extract treatment leads to demethylation of CpG residues in the promoter of Oct4 gene. We investigated the methylation status of each CpG in the Oct4 promoter region (10 CpG sites) by sodium bisulphite sequencing [8]. The bisulphite-converted genomic DNA (1µg) from D3, 3T3 and 3T3/D3 (3 weeks post-treatment) cells was amplified for the Oct4 promoter by PCR and PCR products were directly sequenced. As depicted in **Fig. 2A**, upon bisulphite treatment all 10 CpG sites in D3 cells were converted from C to T, indicating the unmethylated status of Oct4 promoter in this murine ESC cell line (open circles). All 10 sites were methylated in 3T3 cells (closed circles), however, treatment of 3T3 cells with D3

extracts led to de-methylation at 8/10 CpG residues in 3T3/D3 cells. The D3-extract induced Oct4 promoter demethylation in the 3T3/D3 cells was independently corroborated by restriction enzyme analysis. In the Oct4 promoter region, there is one HpyCH4IV (methylated CpG specific restriction enzyme) site at –202. We analyzed the DNA methylation status of the –202 site by HpyCH4IV restriction analysis in D3, 3T3 and 3T3/D3 cells. A ~250bp promoter region including site –202 of mouse Oct4 was amplified by PCR from the bisulphite treated genomic DNA from all three cell types. As shown in **Fig 2B**, the PCR product was not digested with HpyCH4IV in D3 cells, indicating that the genomic DNA of D3 cells was unmethylated at this particular Oct4 promoter site. In contrast, the PCR product was readily digested in 3T3 cells indicating methylation of the Oct4 –202 CpG site. Interestingly, the PCR product from 3T3/D3 cells was resistant to digestion by HypCH4IV, suggesting that treatment of 3T3 cells with D3 extracts induced de-methylation of CpG sites thereby reversing the repression of Oct4 mRNA expression, observed in 3T3 cells.

DNA methylation/demethylation and dependent gene suppression/activation is coupled with modifications to the histone proteins, which together lead to chromatin remodeling and new patterns of gene expression[23, 24]. Therefore, we further confirmed the D3-extract induced epigenetic changes by assessing the acetylation of histones (H) 3 and 4 and methylation status of lysine 9 (K9) residue in histone 3 protein within Oct4 promoter by Chromatin Immunoprecipitation (ChIP) assays[25] using specific antibodies. The Oct4 promoter was amplified from immunoprecipitated chromatin DNA by PCR. ChIP analyses showed that the promoter of Oct4 had increased acetylation of H3 and H4 (**Fig. 2C**) and decreased dimethylation of K9-histone 3 (**Fig. 2D**) in 3T3/D3 cells compared to 3T3 cells. Together these data suggest that D3-extract induced de-differentiation and nuclear re-programming of 3T3/D3 cells is mediated, at least in part, by chromatin remodeling leading to the activation of Oct4. Considering that DNA methylation and histone modifications are involved in various

biological phenomena, such as tissue-specific gene expression, cell differentiation, X-chromosome inactivation, genomic imprinting, changes in chromatin structure, and tumorogenesis[26-34], it is conceivable that the changes in Oct4 promoter CpG methylation and histone modifications by exposure of 3T3 cells to ESC extracts, may be one of the principal epigenetic events underlying de-differentiation and activation of ESC specific genes in 3T3 cells.

D3-extract treatment induces genome-wide gene expression profile changes in re-programmed NIH3T3 cells

To gain further insights into the changes in gene expression patterns in reprogrammed 3T3/D3 cells, we performed global gene-expression profiles of D3, 3T3 and 3T3/D3 using Affymetrix mouse genome 2A gene chips. Differentially expressed genes between the three cell types 3T3, D3, and 3T3/D3 were determined by a simple one-way ANOVA performed on the RMA expression values of each probe set, using the R package limma[35]. A multiple testing adjustment[36] was performed on the resulting statistics to adjust the false discovery rate. Differentially expressed probes with adjusted *p*-value < 0.001 and a fold-change of greater than 2 (absolute log fold change of > than 1) were extracted for further inspection. This resulted in 3,286 probes with statistically significant differential expression between cell types 3T3 and 3T3/D3 including the significant up-regulation of ESC specific genes and down-regulation of somatic genes. Hierarchical clustering, using the Pearson correlation coefficient and average agglomeration method, was performed on the 3,286 genes (2187 down-regulated genes and 1099 up-regulated genes) that were differentially expressed between 3T3 and D3/3T3 cells. The heatmap in **Fig. 3A** of z-scored probes illustrates this clustering, in which z-scores (subtraction of mean and division by standard deviation of normalized values) were computed for each probe across all 9 arrays. The expression pattern of a subset of 99 significantly up-regulated

genes in 3T3/D3 cells, including Oct4 and nanog, was similar in D3 cells (**Fig.3B**). The expression levels of representative up-regulated and down-regulated genes observed in gene chip experiments were independently confirmed by real-time RT-PCR which showed similar upregulation of ESC specific transcripts and down-regulation of somatic transcripts (**Fig. 3C**). A list of selected genes, their relative expression level and functional description is depicted in **supplementary Table S1** and functional grouping of all 3,286 genes found to be differentially expressed between 3T3 and 3T3/D3 cell types is shown in **supplementary Fig. S3**.

Re-programmed 3T3/D3 cells re-differentiate into cells of multiple lineage

We next determined the re-differentiation potential of de-differentiated 3T3/D3 cells into multiple cell types both *in vitro.* Under culture conditions conducive for cell-type specific differentiation, 3T3/D3 cells acquired protein expression specific to neuronal, endothelial (EC), cardiomyocyte (CMC) and adipocyte cells (**Fig 4A**). Cell-type specific mRNA expression analysis (**Fig.4B,C**) and morphological appearance (see **Supplementary Fig.S4** online) further confirmed EC and CMC differentiation.

Transplantation of re-programmed 3T3 cells into surgically induced mouse hind limb ischemia model improves functional and anatomical blood repair.

To ascertain the functional efficacy of reprogrammed cells in a physiologically relevant model of tissue repair, we conducted cell transplantation studies in a well-established mouse hind limb ischemia model described in our prior publication[25]. Immediately following the surgery, mice were assigned to two groups (n=15 each) and 3T3/D3 or 3T3 cells ($2X10^5$), labeled with DiI for tracing purposes, were injected into the ischemic muscles at 3 different sites. Physiological blood flow

recovery was assessed by Laser Doppler Perfusion Imaging (LDPI) on days 7, 10 and 14 (n=5 each time point) post- surgery, in both groups of mice. As shown in representative perfusion images in **Fig. 5A** and quantified as the ratio of blood flow in ischemic to non-ischemic limb, in **Fig. 5B**, mice transplanted with 3T3/D3 cells, displayed significantly improved perfusion in the ischemic limb at all time points compared to mice treated with 3T3 control cells ($p<0.01$). Tissue sections from ischemic hind limbs were stained with mouse FITC-labeled anti-isolectinB4 (IB4) and anti-desmin antibodies todetrmine differentiation of transplanted cells. Fluorescent microscopy was conducted to visualize IB4+ (green) and DiI+ (red) cells and desmin+ (green) and DiI+ (red) cells to determine EC and muscle differentiation, respectively, of transplanted cells and images in the same visual field were merged to generate composite image. As shown in **Fig. 5D** many IB4+DiI double positive cells (indicated by yellow fluroscence) were observed in the ischemic tissue of mice treated with 3T3/D3 cells (panel b) compared to those treated with control 3T3 cells (panel a). Similarly, a large number of 3T3/D3 cells co-expressed muscle marker, desmin, in the ischemic hind limbs while very few desmin+DiI double positive cells in control 3T3 treated mice were observed (**Fig. 5D**, panels c and d). Similar patterns were observed when tissue sections were stained with additional EC and muscle cell markers (CD31 and alpha-smooth muscle actin; see **supplementary Fig. S5 online**) Taken together, these data suggest that re-programmed somatic cells are capable of multi-lineage differentiation in vivo and participate in the functional tissue repair and regeneration.

Intra-cardiac transplantation of 3T3/D3 cells improves left ventricular functions after myocardial infarction

Functional efficacy of 3T3/D3 cells in tissue repair was also tested in a model of acute myocardial infarction (AMI). Mice underwent surgery to induce AMI by ligation of the left anterior descending

coronary artery, as described[38]. Animals were sub-divided into 3 groups (10 each), and received intramyocardial injection of $5X10^4$ lentiviral-GFP transduced (to track transplanted cells up to 4 weeks, in vivo) 3T3/D3 or 3T3 control cells or saline, respectively, in a total volume of 10µl at 5 sites (basal anterior, mid anterior, mid lateral, apical anterior and apical lateral) in the peri-infarct area. Left ventricular function was assessed by transthoracic echocardiography (SONOS 5500, Hewlett Packard) as described[38,39]. We performed physiological assessment of the left ventricular (LV) function after AMI in all groups of mice at basal level before surgery and on days 7, 14 and 28, post-AMI). Left ventricular end-diastolic areas (LVEDA) were similar in the 3T3 cell and saline groups before and at all time points after AMI (**Fig. 6A**, red and grey lines, respectively). In contrast, however, mice treated with the 3T3/D3 cells revealed less ventricular dilation (**Fig. 6A** blue line, $p< 0.05$ in 3T3/D3 vs. control groups). Additionally, fractional shortening (FS), an indicator of contractile function, was consistently depressed in mice receiving saline and control 3T3 cells (**Fig. 6B**). However, treatment with 3T3/D3 cells significantly improved FS at all time points tested (at 4 weeks post-surgery, $p< 0.01$ vs. saline group and $p<0.05$ vs. control 3T3 cell treated group). The individual values for evaluated LV function parameters at various time points are shown in **Supplementary Table S2 online**. Gains in post-AMI physiological heart function in mice transplanted with D3-extract treated 3T3 cells were further corroborated by histological evaluation of hearts from each group of mice. As shown in **Fig. 6C**, the fibrosis areas in mouse hearts receiving either saline or control 3T3 cells were significantly larger than in mice that received 3T3/D3 cells ($p<0.001$). Tissue sections were also stained with BS1 lectin to determine the capillary density at the border zone of the infarcted myocardium. Significantly higher capillary density was observed in the mice receiving 3T3/D3 cells than in mice receiving control 3T3 cells or saline (**Fig. 6D**, $p<0.01$).

Immuno-fluorescence staining on myocardial sections was performed to determine CMC and EC differentiation of the transplanted (GFP+) cells. EC differentiation of transplanted cells was investigated by co-expression of GFP+CD31 by transplanted cells. As shown in **Fig. 6E** (panels a,b), GFP+CD31 double positive cells were observed in myocardial sections obtained from mice transplanted with 3T3/D3 cells, while sections obtained from control 3T3 transplanted hearts did not show the evidence for EC differentiation. To evaluate the CMC differentiation of the transplanted cells in the myocardium, tissue sections were stained with a specific CMC marker, connexin43, and the GFP+ cells (3T3 or 3T3/D3; green) co-expressing connexin43 (red) were visualized as double positive (yellow) cells in the merged images. As shown in **Fig. 6E** (panels c,d), GFP + connexin43 double positive cells (yellow fluorescence) were observed in mice treated with 3T3/D3 cells, suggesting that some of the transplanted cells differentiated into CMC lineage in vivo, while no evidence of CMC differentiation was observed for transplanted 3T3 cells. Immunofluoresence staining of additional CMC specific marker cardiotroponin I, further corroborated CMC differentiation of 3T3/D3 cells (**see Supplementary Fig. S6A, online**). Transplantation of 3T3/D3 cells also led to decreased apoptosis and increased cellular proliferation in the ischemic myocardium as assessed by TUNEL positive and Ki67 positive nuclei, respectively (**see supplementary Fig. S6B, online**).

DISCUSSION

The goal of therapeutic cloning is to produce pluripotent stem cells with the nuclear genome of the patient and induce the cells to differentiate into replacement cells, for example, CMCs for repairing damaged heart tissue. Reports on the generation of pluripotent stem cells[12-14] or histocompatible tissues[39] by nuclear transplantation, and on the correction of a genetic defect in cloned ESCs[40],

suggest that therapeutic cloning could, in theory, provide a source of cells for regenerative therapy. Recent evidence on the efficacy of human therapeutic cloning, however, underscores the difficulties associated with the generation of human ESC lines for therapeutic purposes. Moreover, a number of limitations may hinder the strategy of therapeutic cloning for future clinical applications. Extremely low efficiency of somatic nuclear transfer is a major concern[41]. Analysis of the literature on mouse SNT derived ESC lines raises concerns about the feasibility and relevance of therapeutic cloning, in its current embodiment, for human clinical practice[41-43]. This limitation might be alleviated with oocytes from other species[39] but mitochondrial genome differences between species are likely to pose a problem. It is therefore desirable to develop alternative strategies to oocyte-dependent autologous stem cell generation. Our data indicating mESC extract-mediated reverse de-differentiation of terminally differentiated murine fibroblasts and multi-lineage re-differentiation of these reprogrammed cells not only support the feasibility of such an approach but more importantly, provide evidence that the stem-like cells obtained using this methodology are functionally competent for tissue repair.

Oocyte-independent epigenetic re-programming of somatic cell by somatic-ES cell fusion reported by several recent studies has generated a lot of enthusiasm[9,10] . However, this strategy, although excellent for mechanistic studies, retains certain drawbacks that are associated with oocyte-dependent therapeutic cloning. Firstly, the 2 cells used to generate hybrid cells are not derived from autologous source, secondly the efficiency of fusion remains low (1-3/1000), thirdly the genetic stability of heterokaryon hybrids remains to be established:- one will have to devise the technological innovations to delete additional set of chromosomes, and finally the efficacy of reprogrammed cell to retain the ES like properties if ES cell derived nucleus is removed remains to be elucidated. Recently,

a major breakthrough was reported whereby forced expression of transcription factors Oct4, Sox2, c-Myc and Klf4 was shown to induce pluripotency in fibroblasts (designated as induced pluripotent stem (iPS) cells), although with a low efficiency[44]. The iPS cells were isolated by selection for activation of Fbx15, which is a downstream gene of Oct4. This important study, however, left a number of questions unresolved: (1) although iPS cells were pluripotent they were not identical to ES cells (for example, iPS cells injected into blastocysts generated abnormal chimaeric embryos that did not survive to term); (2) gene expression profiling revealed major differences between iPS cells and ES cells; (3) because the four transcription factors were transduced by constitutively expressed retroviral vectors it was unclear why the cells could be induced to differentiate and whether continuous vector expression was required for the maintenance of the pluripotent state; and (4) the epigenetic state of the endogenous pluripotency genes Oct4 and Nanog was incompletely reprogrammed, raising questions about the stability of the pluripotent state.

Our observations demonstrating that mESC protein extracts can reprogram somatic cells towards multipotency, would argue that multipotent epigenome could be activated in somatic cells without fusion and forced expression of nucleic acids. More importantly, our's is the first study to demonstrate that transplantation of de-differentiated somatic cells can repair ischemic tissue and mediate gain in physiological functions in relevant models of tissue injury. Taken together our biochemical, molecular and functional data provide an oocyte- independent approach for the generation of functional autologous multipotent cells from terminally differentiated somatic cells. The refinement of techniques and additional experimental data to elucidate applicability of this approach in primary somatic cells of different lineages and derivation of single cell clones displaying stable, long-term reprogramming may hold significant promise for future use of such generated cells in regenerative medicine, including cardiac repair and regeneration.

METHODS

Cell culture. NIH3T3 Swiss-Albino fibroblasts (ATCC) were cultured in DMEM (Sigma-Aldrich) with 10% FCS, L-glutamine, and 0.1 mM β-mercaptoethanol. The D3-mESC were obtained from ATCC and cultured as described earlier[45].

Cell Extracts. The mESC and 3T3 cell extracts were prepared as described previously[22]. Briefly, the cells were washed in phosphate-buffered saline (PBS) and in cell lysis buffer (100 mM HEPES, pH 8.2, 50 mM NaCl, 5 mM $MgCl_2$, 1 mM dithiothreitol, and protease inhibitors), sediment at 10,000 rpm, re-suspended in 1 volume of cold cell lysis buffer, and incubated for 30–45 min on ice. Cells were sonicated on ice in 200-µl aliquots using a sonicator fitted with a 3-mm-diameter probe until all cells and nuclei were lysed, as judged by microscopy. The lysate was sedimented at 12,000 rpm for 15 min at 4°C to pellet the coarse material. The supernatant was aliquoted, frozen in liquid nitrogen and stored at -80°C. Protein concentration of the mESC and NIH3T3 cell extracts were determined by Bradford assay.

Streptolysin –O (SLO)-mediated Permeabilization and Cell Extract Treatment. NIH3T3 cells were washed in cold PBS and in cold Ca^{2+}- and Mg^{2+}-free Hank's balanced salt solution (HBSS) (Invitrogen, Carlsbad, CA). Cells were re-suspended in aliquots of 100,000-cells/100 µl of HBSS, or multiples thereof; placed in 1.5-ml tubes; and centrifuged at 1500 rpm for 5 min at 4°C. After sedimentation, cells were suspended in 97.7 µl of cold HBSS, tubes were placed in a H_2O bath at 37°C for 2 min, and 2.3 µl of SLO (Sigma-Aldrich) (100 µg/ml stock diluted 1:10 in cold HBSS) was added to a final SLO concentration of 230 ng/ml. Samples were incubated horizontally in a H_2O bath for 50 min at 37°C with occasional agitation and set on ice. Samples were diluted with 200 µl of cold HBSS and cells were collected by sedimentation at 1500 rpm for 5 min at 4°C. Permeabilization

efficiency of >80% was obtained as assessed by monitoring uptake of a 70,000-M_r Texas Red-conjugated dextran (50 μg/ml; Invitrogen). After permeabilization, NIH3T3 cells were suspended at 2000 cells/μl in 100 μl of mESC extract or control NIH3T3 cells extract containing an ATP-regenerating system (1 mM ATP, 10 mM creatine phosphate, and 25 μg/ml creatine kinase; Sigma-Aldrich), 100 μM GTP (Sigma-Aldrich), and 1 mM each nucleotide triphosphate (NTP; Roche Diagnostics, Indianapolis, IN). The cells were incubated for 1 hr at 37°C in a H_2O bath with occasional agitation. To reseal plasma membranes, the cell suspension was diluted with complete DMEM medium containing 2 mM $CaCl_2$, antibiotics and cells were seeded at 100,000 cells per well on a 48-well plate. After 2 hrs, floating cells were removed, and cells were cultured in D3 maintenance medium.

Determination of de-differentiation. De-differentiation of NIH3T3 following D3-cell extract treatment was determined by the induction of ESC markers both at mRNA level by quantitative real time PCR and at protein level by immuno-staining. Total cellular RNA was harvested at various time points and the quantitative real-time RT-PCR was performed to determine mRNA expression of selected embryonic stem cell markers in self extract and D3-extract treated cells, as described previously[45,46]. Relative mRNA expression of target genes was normalized to the endogenous 18S control gene (Applied Biosystems). Induction of embryonic stem cell specific mRNAs was further corroborated by immunofluorescence protein staining of induced specific stem cell markers in NIH3T3 cells treated with D3 extract. For immuno-staining, both control and D3 extract treated NIH3T3 cells were cultured in medium in the absence and presence of LIF for 10 days. Then the cells were harvested and cultured 1 X 10^4 cells per well in 4-well slides coated with 0.5% gelatin for another 2 days. The slides were stained with specific antibodies to stem cell markers, c-Kit, SSEA1

and Oct-4. De-differentiation was also determined by the lamin B and lamin A/C (markers of soma) protein expression.

CMCs and EC lineage differentiation of 3T3/D3 cells. To determine the re-differentiation potency of dedifferentiated 3T3/D3 cells into cardiomyocytes, cells were cultured in complete DMEM containing 5 ng/ml of LIF and 3 ng/ml of Bone morphogenic protein –2 (BMP2) in 6-well culture plates (1 X 10^6 cells per well) and 4-well chamber slides (1 X 10^4 cells per well) coated with 0.5% gelatin for 7 days[45]. Total cellular RNA was harvested from 6-well culture plate and used to analyze quantitative mRNA expression of CMC specific markers, cardiotroponin I and T, connexin 43, GATA4, Mef2c, Nkx2.5 and Tbx5. The expression was normalized to that of 18S RNA. The protein expression of was determined by immunochemical staining. For EC lineage differentiation, cells were cultured in endothelial differentiation medium (10% FBS/EBM-2; Clonetics) medium containing supplements (SingleQuot Kit; Clonetics) for 7 days. mRNA expression for EC markers, CD31 and Flk1 was determined by real-time PCR and by incubation with DiI-acLDL (Biomedical Technologies) for one hour followed by Isolectin B4 staining. The dual stained cells were considered endothelial cells.

Induction of neuronal and adipogenic differentiation. The neuronal differentiation was performed as described earlier[47]. Briefly, cells were seeded in complete DMEM medium at 5 × 10^5 cells per 90-mm sterile culture dish. Suspension cultures were maintained for 24 hrs before adding 10 μM all-*trans*-retinoic acid (Sigma-Aldrich). Cells were cultured for 3 wks in retinoic acid, replacing the medium every 2–3 days. Subsequently, cell aggregates were washed in complete DMEM medium and plated onto poly-L-lysine (10 μg/ml; Sigma-Aldrich)-coated plates in complete DMEM medium containing the mitotic inhibitors fluorodeoxyuridine (10 μM; Sigma-Aldrich), cytosine arabinosine

(1 μM; Sigma-Aldrich), and uridine (10 μM; Sigma-Aldrich). The culture dishes were stained for neuronal markers nestin and β-tubulin-III. The adipogenic differentiation was performed as described elsewhere[48]. Briefly, the cells were cultured for 21 days in complete DMEM/Ham's F-12 medium containing dexamethasone, insulin and indomethacin. Cells were fixed with 4% paraformaldehyde, washed in 5% isopropanol, and stained for 15 min with Oil-Red-O (Sigma Aldrich).

Immunochemical staining. For immunochemical staining, cells under different culture conditions were cultured on 4 well slides for indicated time, rinsed once with PBS and fixed with 4% paraformaldehyde (Sigma) in PBS for 30 min. The slides were again rinsed three times with PBS and then permeabilized with 0.3% of Triton X-100 (Sigma) in PBS for 5 min. After 2 washes with PBS, specific primary antibodies diluted in PBS containing 1% FBS were added and incubated overnight at 4°C. After 3 washes with PBS, the slides were incubated with respective secondary antibodies for 1 hr at 37°C. The excess secondary Abs on the slides were rinsed off with PBS three times. Finally, to visualize nuclei, slides were stained with DAPI for 5 min, washed 3 times with PBS, allowed to dry for 5 min and then mounted on Vectashield mounting medium for fluorescence imaging. The photographs were taken in a Nikon TE200 Digital Imaging system.

Determination of Oct4 promoter methylation, bisulfite genomic sequencing and Chromatin Immunoprecipitation (ChIP). Genomic DNA prepared from D3, 3T3/D3 and 3T3 cells was amplified for the Oct4 promoter and the PCR product was digested with HpyCH4IV restriction enzymes that only cleave at methylated CpG sites. The digested products were analyzed on agarose gels. For genomic bisulphate sequencing, genomic DNA from cells was digested with EcoR1 and

was used for bisulphite treatment using an EZ DNA methylation-Gold kit essentially following the manufacturer's instructions. The treated DNA was ethanol-precipitated and resuspended in water and then amplified by PCR using mouse methylation specific Oct4 primers PCR products were digested with the HpyCH4IV (New England Biolabs) restriction enzyme. Because only unmethylated cytosine residues were changed to thymines by the sodium bisulphite reaction, PCR fragments from nonmethylated genomic DNA were resistant to HpyCH4IV, and those from methylated DNA were digested by the enzymes. The resultant products of restriction mapping were assessed by agarose gel electrophoresis. The Remaining PCR products were purified through the Wizard DNA Clean-Up system (Promega, Madison, WI), and were directly sequenced to determine the methylation status of all 10 CpG residues present in the amplified promoter region. Chromatin Immunoprecipitation (ChIP) assays were performed essentially as described in our recent publication[25]. Anti-Acetyl H3, anti-acetyl H4 and anti-dimethyl K9 antibodies were purchased from Upstate Biotech and Santa Cruz.

Genome-wide expression profiling and gene expression analyses. Affymetrix mouse genome A2 GeneChips were used for hybridization. Using a poly-dT primer with a incorporated T7 promoter, double-stranded cDNA was synthesized from 5 μg total RNA using a double-stranded cDNA synthesis kit (Invitrogen, Carlsbad, CA). Double-stranded cDNA was purified with the Affymetrix sample cleanup module (Affymetrix, Santa Clara, CA). Biotin–labeled cRNA was generated from the double-stranded cDNA template though in-vitro transcription with T7 polymerase, and a nucleotide mix containing biotinylated UTP (3'-Amplification Reagents for IVT Labeling Kit; Affymetrix). The biotinylated cRNA was purified using the Affymetrix sample cleanup module. For each sample, 15 μg of IVT product was digested with fragmentation buffer (Affymetrix, Santa

Clara, CA) for 35 minutes at 94°C, to an average size of 35 to 200 bases. 10 μg of the fragmented, biotinylated cRNA, along with hybridization controls (Affymetrix), was hybridized to a Mouse 430A 2.0 GeneChip for 16 hours at 45°C and 60 rpm. Arrays were washed and stained according to the standard Antibody Amplification for Eukaryotic Targets protocol (Affymetrix). The stained arrays were scanned at 532 nm using an Affymetrix GeneChip Scanner 3000.

During analysis and for quality control, GeneChip® arrays were first inspected using a series of quality control steps. Present call rates were consistent across the arrays, ranging from 56% to 63%. The hybridization controls (BioB, BioC, Cre) were found to be present 100% of the time. Images of all arrays were examined, and no obvious scratches or spatial variation was observed. A visual inspection of the distribution of raw PM probe values for the twelve arrays showed no outlying arrays. Similarly, digestion curves describing trends in RNA degradation between the 5' end and the 3' end of each probeset were generated, and all twelve proved comparable. Probe sets with no present calls across the twelve arrays as well as Affymetrix control probe sets were excluded from further analyses. Raw intensity values for the remaining 17,213 probe sets were processed first by RMA (Robust Multi-Array Average) using the R package affy[46]. Specifically, expression values were computed from raw *CEL* files by first applying the RMA model of probe-specific correction of PM (perfect match) probes. These corrected probe values were then normalized via quantile normalization, and a median polish was applied to compute one expression measure from all probe values. Resulting RMA expression values were $\log_2$-transformed. (Please see the affy manual at www.bioconductor.org/repository/devel/vignette/affy.pdf for details). Distributions of expression values processed via RMA of all arrays were very similar with no apparent outlying arrays. Pearson correlation coefficients and Spearman rank coefficients were computed on the RMA expression

values (log_2-transformed) for each set of biological triplicates. Spearman coefficients ranged from .990 to .996; Pearson coefficients ranged between 0.991 and 0.997. Differential expression of genes was determined by one-way ANOVA on the RMA expression values of each probe set, using the R package limma[35]. A multiple testing adjustment[36] was performed on the resulting statistics to adjust the false discovery rate. Differentially expressed probes with adjusted *p*-values < 0.01 and a fold-change of greater than two (absolute log fold change of greater than 1) were extracted for further inspection. Hierarchical clustering was obtained by using the Pearson correlation coefficient and an average agglomeration method, and the heatmaps were generated using z-scored probes, in which z-scores (subtraction of mean and division by standard deviation of normalized values) were computed for each probe across all twelve arrays.

GFP- transduction and DiI labeling of cells for transplantation. For tracking of transplanted cells in AMI model, cells were transduced with a lentivirus-GFP construct. For tracking of transplanted cells in hind limb ischemic tissues, the cells were labeled with DiI before the transplantation[25].

Hind limb ischemia, cell transplantation, and laser Doppler imaging and histology. All procedures were performed in accordance with the guidelines of the Institutional Animal Care and Use Committee. The hind limb ischemia was established by the excision of femoral artery in the left hind limb in 10 male 8-week- old mice (Jackson Labs) essentially as described in our prior publication[25]. The animals were grouped into 2 (n=15/group), each receiving either a total of DiI-labeled- $5X10^4$ 3T3 cells or 3T3-D3 cells at multiple sites into the ischemic muscle. Laser Doppler imaging to determine blood flow was performed immediately after surgery (day 0) and at days 7, 10

and 14 after cell injections. Fourteen days after cell transplantation, the tissues were harvested and assayed by histochemical/immuno-fluorescence staining for isolectin B4, CD31 (EC identity), Desmin, alpha-SMA (muscle), and DiI followed by fluorescence microscopy. In some experiments, animals were perfused with FITC–BS-1 lectin to identify capillaries before sacrifice and tissue retrieval.

Mice and establishment of AMI. The study involved 8-week-old male FVB mice (n=30; Jackson Laboratories). Mice underwent surgery to induce acute myocardial infarction by ligation of the left anterior descending coronary artery, as described before[37,49]. Animals were sub-divided into 3 groups and received intramyocardial injection of $5X10^4$ lentiviral-GFP transduced D3-extract treated cells, 3T3 fibroblast control cells and saline, respectively, in total volume of 10µl at 5 sites (basal anterior, mid anterior, mid lateral, apical anterior and apical lateral) in the peri-infarct area.

Physiological assessments of LV function and histology. Mice underwent echocardiography just before MI (base level) and one, two and four weeks after AMI as described before[37, 38]. Briefly, transthoracic echocardiography was performed with a 6 to 15 MHz transducer (SONOS 5500, Hewlett Packard). Two-dimensional images were obtained in the parasternal long and short axis and apical 4-chamber views. M-mode images of the left ventricular short axis were taken just below the level of the mid-papillary muscles. Left ventricular end-diastolic and end-systolic dimensions were measured and functional shorting was determined according to the modified American Society of Echocardiography-recommended guidelines. A mean value of 3 measurements was determined for each sample. On day 28 post-AMI, Mice were euthanized and the aortas were perfused with saline. The hearts were sliced into 4 transverse sections from apex to base and fixed with 4%

paraformaldehyde, methanol or frozen in OCT compound and sectioned into 5-μm thickness. Immunofluorescence staining was performed to determine CMC and EC differentiation of transplanted cells. For the measurement of fibrosis, tissues sections were frozen in OCT compound and sectioned for elastic tissue/trichrome to measure the average ratio of the external circumference of fibrosis area to LV area.

Statistical analyses.

All experiments were carried out at least 3 times with similar results. Results are presented as mean ± SEM. Comparisons were done by ANOVA (GB-STAT; Dynamic Microsystems Inc.) or χ^2 test for percentages. All tests were 2-sided, and a *P* value of less than 0.05 was considered statistically significant.

ACKNOWLEDGMENTS

Work described in this manuscript was in part supported by American Heart Association grant 0530350N and National Institute of Health grant AA014575 to R.K. and National Institute of Health grants HL63414 to D.W.L. The authors thank Ms. Mickey Neely for secretarial assistance.

AUTHOR CONTRIBUTIONS

J.R., EB and IG were the principal experimentalists. J.R. contributed to the experimental design and execution the writing of the manuscript. H.H. performed animal surgeries and physiological studies. G.Q. made Lentivirus-GFP construct. P.K., D.A. and E.L. performed *in vitro* cell culture experiments and contributed to the writing of the manuscript. K.S. performed genome-wide gene expression profiling and analysis. K.M.R. performed confocal microscope imaging. Y.Z. and D.W.L. provided critical discussion and helped writing and editing of the manuscript. R.K. conceptualized, designed and coordinated the project and contributed to the writing/editing of the manuscript.

COMPETING INTERESTS STATEMENTS

The authors declare no competing financial interests.

REFERENCES

1. Losordo, D.W. & Dimmeler, S. Therapeutic angiogenesis and vasculogenesis for ischemic disease: part II: cell-based therapies. *Circulation* **109**, 2692-2697 (2004).
2. Dimmeler, S. ATVB in focus: novel mediators and mechanisms in angiogenesis and vasculogenesis. *Arterioscler. Thromb. Vasc. Biol.* **11**, 2245 (2005).
3. Walter, D.H. *et al.* Impaired CXCR4 signaling contributes to the reduced neovascularization capacity of endothelial progenitor cells from patients with coronary artery disease. *Circ. Res.* **97**, 1142-1151 (2005).
4. Urbich, C. & Dimmeler, S. Risk factors for coronary artery disease, circulating endothelial progenitor cells, and the role of HMG-CoA reductase inhibitors. *Kidney Int.* **67**, 1672-1676 (2005).
5. Tepper, O.M. *et al*. Human endothelial progenitor cells from type II diabetics exhibit impaired proliferation, adhesion, and incorporation into vascular structures. *Circulation* **106**, 2781-2786 (2002).
6. Ii, M. *et al*. Endothelial progenitor thrombospondin-1 mediates diabetes-induced delay in reendothelialization following arterial injury. *Circ. Res.* **98**, 697-704 (2006).
7. Byrne, J.A., Simonsson, S., Western, P.S. & Gurdon, J.B. Nuclei of adult mammalian somatic cells are directly reprogrammed to oct-4 stem cell gene expression by amphibian oocytes. *Curr Biol.* **13**, 1206-1213 (2003).
8. Yamanaka, S. Strategies and new developments in the generation of patient-specific pluripotent stem cells. Cell Stemm Cell **1**, 39-49 (2007).
9. Tada, M., Takahama, Y., Abe, K., Nakastuji, N. & Tada, T. Nuclear reprogramming of somatic cells by in vitro hybridization with ES cells. *Curr. Biol.* **11**, 1553-1558 (2001).
10. Cowan, C.A., Atienza, J., Melton, D.A. & Eggan, K. Nuclear reprogramming of somatic cells after fusion with human embryonic stem cells. S*cience* **309***,* 1369-1373 (2005).
11. Gurdon, J.B. & Byrne, J.A. The first half-century of nuclear transplantation. *Proc. Natl. Acad. Sci. USA.* **100**, 8048-8052 (2003).

12. Cibelli, J.B. *et al*. Transgenic bovine chimeric offspring produced from somatic cell-derived stem-like cells. *Nat. Biotechnol.* **16**, 642-646 (1998).
13. Munsie, M.J. *et al*. Isolation of pluripotent embryonic stem cells from reprogrammed adult mouse somatic cell nuclei. *Curr Biol*. **10**, 989-992 (2000).
14. Wakayama, T. *et al*. Differentiation of embryonic stem cell lines generated from adult somatic cells by nuclear transfer. *Science* **292**, 740-743 (2001).
15. Hwang, W.S., Lee, B.C., Lee, C.K. & Kang, S.K. Human embryonic stem cells and therapeutic cloning. *J. Vet. Sci*. **6**, 87-96 (2005).
16. Gaustad, K.G., Boquest, A.C., Anderson, B.E., Gerdes, A.M. & Collas, P. Differentiation of human adipose tissue stem cells using extracts of rat cardiomyocytes. *Biochem Biophys Res Commun.* **314**, 420-427 (2004).
17. Håkelien, A.M. *et al*. Long-term in vitro, cell-type-specific genome-wide reprogramming of gene expression. *Exp. Cell Res.* **309**, 32-47 (2005).
18. Landsverk, H.B. *et al*. Reprogrammed gene expression in a somatic cell-free extract. *EMBO Rep.* **3**, 384-389 (2002).
19. McGann, C.J., Odelberg, S.J. & Keating, M.T. Mammalian myotube dedifferentiation induced by newt regeneration extract. *Proc. Natl. Acad. Sci. USA*. **98**, 13699-13704 (2001).
20. Hansis, C., Barreto, G., Maltry, N. & Niehrs, C. Nuclear reprogramming of human somatic cells by xenopus egg extract requires BRG1. *Curr Biol.* **14**, 1475-1480 (2004).
21. Qin, M., Tai, G., Collas, P., Polak, J.M. & Bishop, A.E. Cell extract-derived differentiation of embryonic stem cells. *Stem Cells* **23**, 712-718 (2005).
22. Taranger, C.K. *et al*. Induction of Dedifferentiation, Genomewide Transcriptional Programming, and Epigenetic Reprogramming by Extracts of Carcinoma and Embryonic Stem Cells. *Mol. Biol. Cell* **16**, 5719-5735 (2005).
23. Trojer, P. & Reinberg, D. Histone Lysine Demethylase and their impact on epigenetics. *Cell* **125**, 213-217 (2006).
24. Klose, R.J. & Bird, A.P. Genomic DNA methylation: the mark and its mediators. Trends Biochem Sci. **31**, 89-97 (2006).
25. Kishore, R. *et al.* The cytoskeletal protein ezrin regulates EC proliferation and angiogenesis via TNF-alpha-induced transcriptional repression of cyclin A. *J. Clin. Invest.* **115**, 1785-1796 (2005).

26. Jones, P.L. *et al*. Methylated DNA and MeCP2 recruit histone deacetylase to repress transcription. *Nat. Genet*. **2**, 187-191 (1998).
27. Cho, J. *et al*. DNA methylation regulates placental lactogen I gene expression. *Endocrinology* **142**, 3389–3396 (2001).
28. Okamoto, K. *et al*. A novel octamer binding transcription factor is differentially expressed in mouse embryonic cells. *Cell* **60**, 461-472 (1990).
29. Rosner, M.H. *et al*. A POU-domain transcription factor in early stem cells and germ cells of the mammalian embryo. *Nature* **345**, 686-92 (1990).
30. Nichols, J. *et al*. Formation of pluripotent stem cells in the mammalian embryo depends on the POU transcription factor Oct4. *Cell* **95**, 379-391 (1998).
31. Niwa, H., Miyazaki, J. & Smith A.G. Quantitative expression of Oct-3/4 defines differentiation, dedifferentiation or self-renewal of ES cells. *Nat. Genet*. **24**, 372-376 (2000).
32. Deb-Rinker, P., Ly, D., Jezierski, A., Sikorska, M. & Walker, P.R. Sequential DNA methylation of the Nanog and Oct-4 upstream regions in human NT2 cells during neuronal differentiation. *J. Biol. Chem.* **280**, 6257-6260 (2005).
33. Nan, X. *et al*. Transcriptional repression by the methyl-CpG-binding protein MeCP2 involves a histone deacetylase complex. *Nature* **393**, 386-389 (1998).
34. Ng, H.H., Jeppesen, P. & Bird, A. Active repression of methylated genes by the chromosomal protein MBD1. *Mol. Cell Biol.* **4**, 1394-406 (2000).
35. Smyth G.K, Gentleman, R., Carey, V., Dudoit, S., Irizarry R. & Huber W. (eds.), Limma: linear models for microarray data. Bioinformatics and Computational Biology Solutions using R and Bioconductor, Springer, New York, p 397-420 (2005).
36. Benjamini, Y., Drai, D., Elmer, G., Kafkafi, N. & Golani I. Controlling the false discovery rate in behavior genetics research. *Behav. Brain Res.* **125**, 133-140 (2001).
37. Iwakura, A. *et al*. Estradiol enhances recovery after myocardial infarction by augmenting incorporation of bone marrow-derived endothelial progenitor cells into sites of ischemia-induced neovascularization via endothelial nitric oxide synthase-mediated activation of matrix metalloproteinase-9. *Circulation* **113**, 1605-1614 (2006).
38. Yoon, Y.S. *et al*. VEGF-C gene therapy augments postnatal lymphangiogenesis and ameliorates secondary lymphedema. *J. Clin. Invest.* **111**, 717-725 (2003).

39. Lanza, R.P., Cibelli, J.B. & West, M.D. Prospects for the use of nuclear transfer in human transplantation. *Nat. Biotechnol*. **17**, 1171-1174 (1999).
40. Rideout, W.M. 3rd, Hochedlinger, K., Kyba, M., Daley, G.Q. & Jaenisch, R. Correction of a genetic defect by nuclear transplantation and combined cell and gene therapy. *Cell* **109**, 17-27 (2002).
41. Mombaerts, P. Therapeutic cloning in the mouse. *Proc. Natl. Acad. Sci. USA*. **100**, 11924-11925 (2003).
42. Cibelli, J.B. *et al*. Parthenogenetic stem cells in nonhuman primates. *Science* **295**, 819 (2002).
43. Humpherys, D. *et al*. Abnormal gene expression in cloned mice derived from embryonic stem cell and cumulus cell nuclei. *Proc. Natl. Acad. Sci. USA*. **99**, 12889-12894 (2002).
44. Takahashi, K. and Yamanaka, S. Induction of Pluripotent Stem Cells from Mouse Embryonic and Adult Fibroblast Cultures by Defined factors. *Cell* **126,** 663-676 (2006).
45. Rajasingh, J. *et al.* STAT3-Dependent Mouse Embryonic Stem Cell Differentiation Into Cardiomyocytes. Analysis of Molecular Signaling and Therapeutic Efficacy of Cardiomyocyte Precommitted mES Transplantation in a Mouse Model of Myocardial Infarction. *Circ Res*. (2007) Sep 6; (Epub ahead of print)
46. Irizarry, R.A., Hobbs, R., Collin, R. & Beazer-Barclay, Y.D. Exploration, normalization, and summaries of high density oligonucleotide array probe level data. *Biostatistics* **4**, 249-264 (2003).
47. Stewart, R., Christie, V.B. & Przyborski, S.A. Manipulation of human pluripotent embryonal carcinoma stem cells and the development of neural subtypes. *Stem Cells* **21**, 248-256 (2003).
48. Boquest, A.C. *et al*. Isolation and transcription profiling of purified uncultured human stromal stem cells: alteration of gene expression after in vitro cell culture. *Mol. Biol. Cell* **3**, 1131-1141 (2005).
49. Kusano, K.F. *et al*. Sonic hedgehog myocardial gene therapy: tissue repair through transient reconstitution of embryonic signaling. *Nat. Med.* **11**, 1197-1204 (2005).

Figure Legends

Figure 1. De-differentiation of mES cell extract treated NIH3T3 cells. NIH3T3 fibroblasts were reversibly permeabilized with SLO and exposed to D3-mESC whole cell extracts or to control self (NIH3T3) extract. Cells were cultured in DMEM supplemented with LIF (10ng/ml) and monitored daily for morphological changes. (**A**) Representative phase contrast image of self-extract treated 3T3 on day 10 (a) and D3-extract treated 3T3 on days 3 (b), 5 (c) and 10 (d). (**B**) Total RNA from 3T3/D3, 4 weeks after initial treatment, was isolated and analyzed for the quantitative mRNA expression by real-time RT-PCR for indicated ESC markers. Data is plotted as fold mRNA expression compared to the mRNA levels in self-extract treated 3T3 cells averaged from 3 similar experiments. (**C**) Cells were cultured on 4 well slides and Oct4 expression was determined by immuno-fluorescence staining. Representative picture is shown. **(D)** Loss of somatic cell marker, lamin A, in 3T3/D3 cells was analyzed by immuno-fluorescence cyto-chemistry and by western blotting (**E**).

Figure 2. D3 extract treatment induces epigenetic changes in 3T3/D3 cells. (**A**) Genomic DNA from indicated cells was digested with EcoRI and was treated with sodium meta-bisulphite. Oct4 promoter was amplified from modified DNA using specific primers by PCR and PCR products were sequenced for the evidence of cytosine conversion to thymine at unmethylated CpG. Filled circle represents methylated CpG and open circles represent unmethylated CpG in Oct4 promoter. (**B**) Oct4 promoter fragment was amplified from bisulphite treated genomic DNA of indicated cells and was subjected to digestion with HypCH4IV restriction enzyme that specifically cleaves methylated CpG. Post-digestion DNA was resolved on 2% ethidium bromide stained gels and photographed. The promoter of Oct4 was analyzed by ChIP for histone H3 and H4 acetylation (**C**) and for

dimethylation status of lysine 9 of histone H3 (**D**). Gels from 3 separate experiments were quantified by NIH image analysis and average values were plotted against levels observed in D3 cells (arbitrarily given a numerical value of 1).

Figure 3. Global gene expression analyses of re-programmed 3T3/D3 cells. (A) Heatmap of z-scored values for 3286 genes showing significant differences ($p<0.001$ and absolute log fold change of >1) between 3T3 and 3T3/D3 cells and the expression level of same genes in D3 cells. (**B**) Heatmap of z-scored 99 genes down-regulated in 3T3 cells and up-regulated in D3 and 3T3/D3 cells. (**C**) Real-time RT-PCR analysis of selected genes up-regulated or down-regulated in re-programmed 3T3/D3 cells.

Figure 4. De-differentiated 3T3/D3 cells differentiate into multiple type cells. (A) Under culture conditions conducive to specific differentiation, 3T3/D3 cells (bottom panels) show protein expression of neuronal (a) CMC (b), endothelial cell (c) and adipocytes (d). (**B**) Quantitative mRNA expression of CMC (B) and EC (C) specific transcripts in 3T3/D3 cells cultured under CMC and EC differentiation conditions. Graph represents average fold mRNA expression from 3 experiments plotted against expression levels in control 3T3 cells.

Figure 5. Transplantation of 3T3/D3 improves recovery of ischemic hind limbs. (A) Representative perfusion imaging of ischemic hind limbs immediately after HLI (left panels) and 14 days post transplantation of either 3T3 (top right panel) or 3T3/D3 (bottom right panel) cells. (**B**) Cumulative perfusion of ischemic hind limbs on various days plotted as the ratio of blood flow in ischemic: non-ischemic limbs. (C) Capillaries in the ischemic limbs were identified as fluorescent

structures (green), stained with in vivo perfusion with FITC-BS-1 lectin. The number of capillaries/per high visual field in different sections was quantified and averaged. **(D)** Differentiation of transplanted 3T3 and 3T3/D3 cells into EC (a, b, respectively) and skeletal muscle cells (b, d, respectively). Merged images of DiI+Isolectin B4 double-positive cells (yellow fluorescence) and DiI+ desmin double positive cells was considered as differentiation into EC and skeletal muscle cell, respectively.

Figure 6. Transplantation of 3T3/D3 cells improves Left Ventricular functions and histological repair in a mouse model of acute myocardial infarction. Transplantation of 3T3/D3 cells significantly improved left ventricular end-diastolic areas (**A**) and left ventricular fractional shortening (**B**) as compared to mice treated with control 3T3 cells and/or saline. **(C)** Quantification of % fibrosis area in 3 groups of mice. (**D**) Quantification of capillary density. Mice were perfused with FITC-BS1 lectin and fluorescently labeled capillaries were counted in 6 randomly selected tissue sections at the border zone from each animal. **(E)** Transplanted 3T3/D3 cells differentiate into EC and CMCs, *in vivo*. Representative merged images (panels a,b) showing co-localization of GFP+ (green) transplanted 3T3 control (a) and 3T3/D3 (b) and EC specific marker, CD31+ (red) cells. Double positive cells are identified by yellow fluorescence in the merged images. Representative merged figures (panels c,d) showing co-localization of GFP+ (green) transplanted control 3T3 cells (c) and 3T3/D3 cells (d) and CMC specific marker, connexin43+ (red) cells. Double positive cells are identified by yellow fluorescence in the merged images.

Figure 1

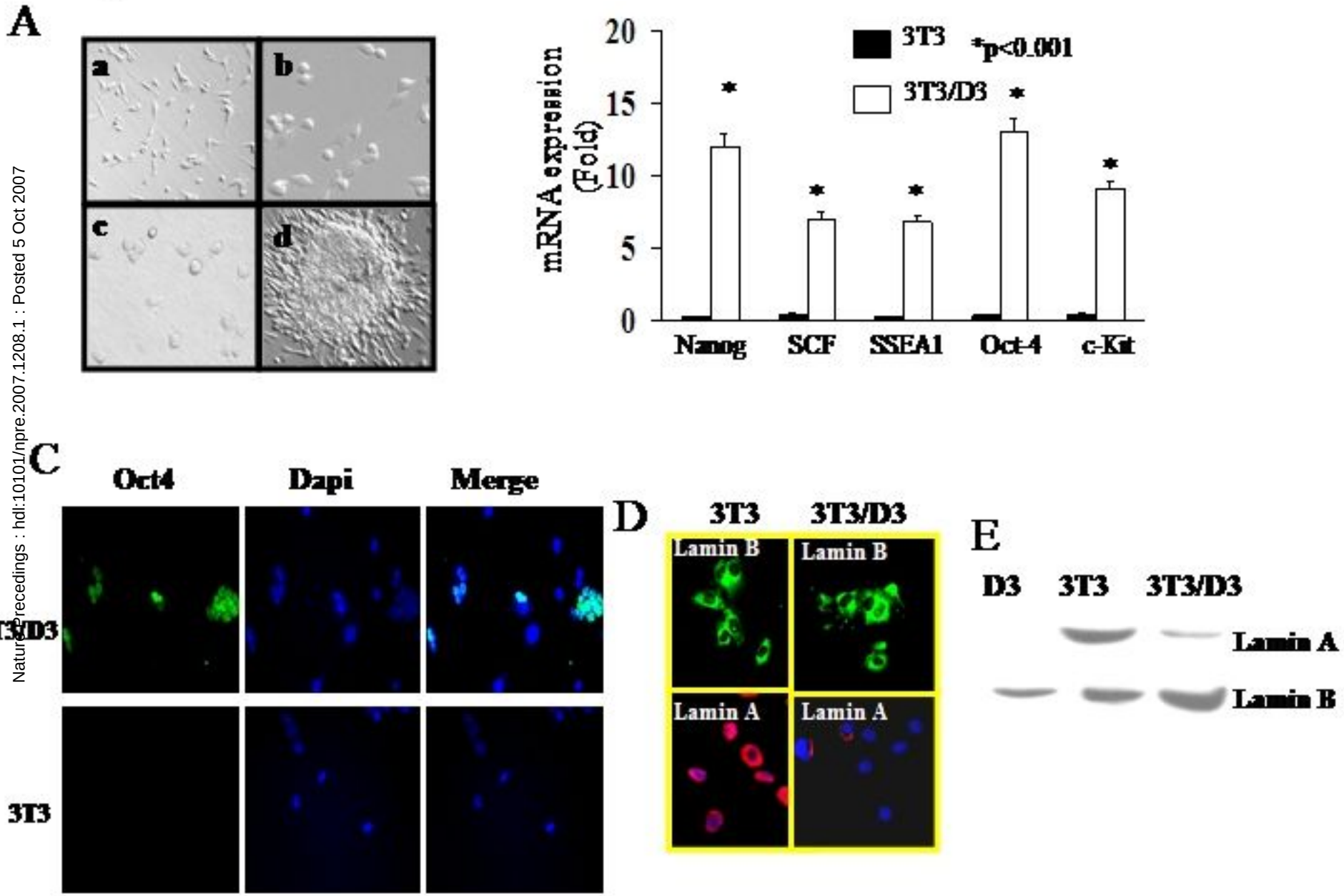

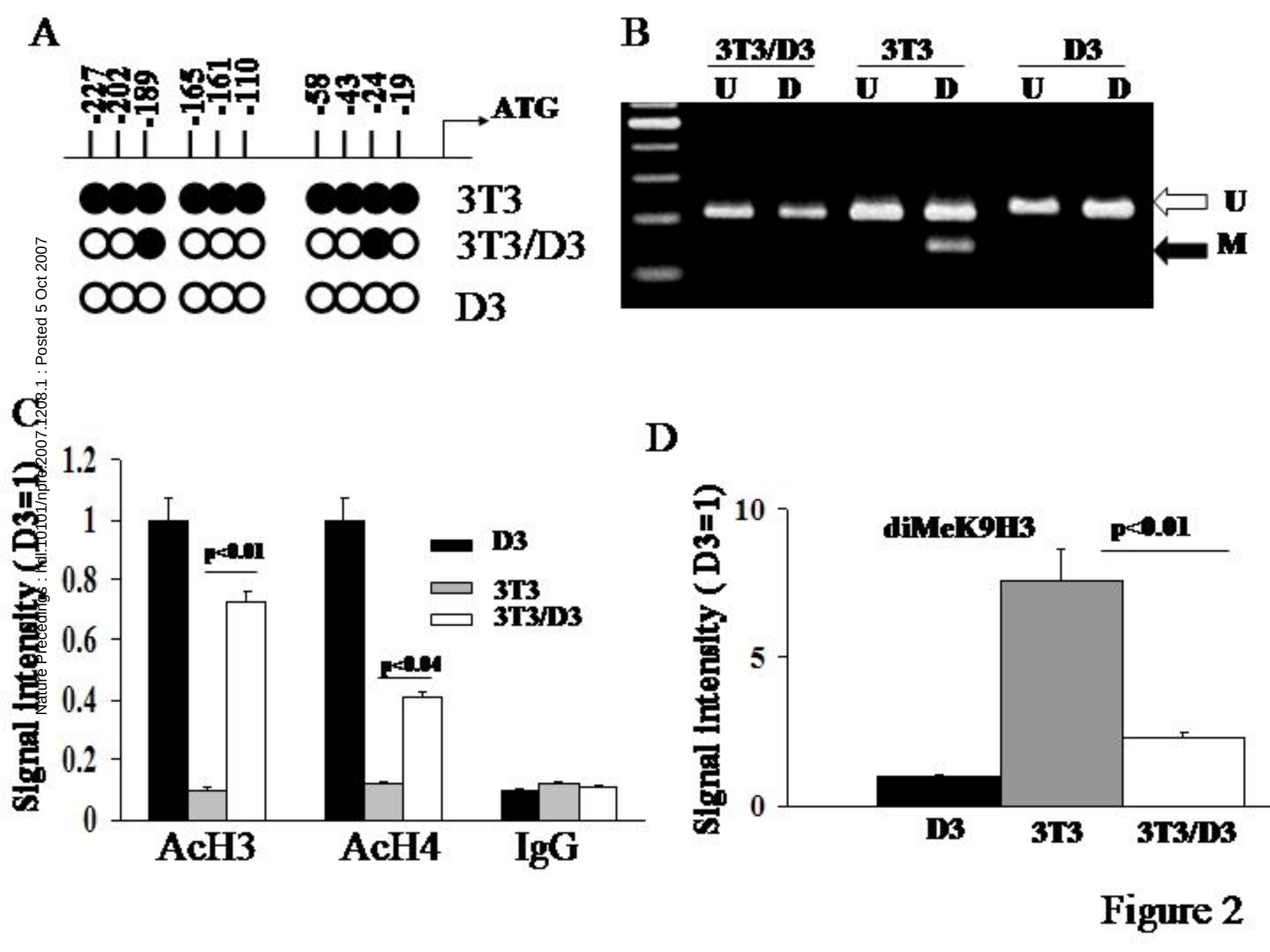

Figure 2

Figure 3

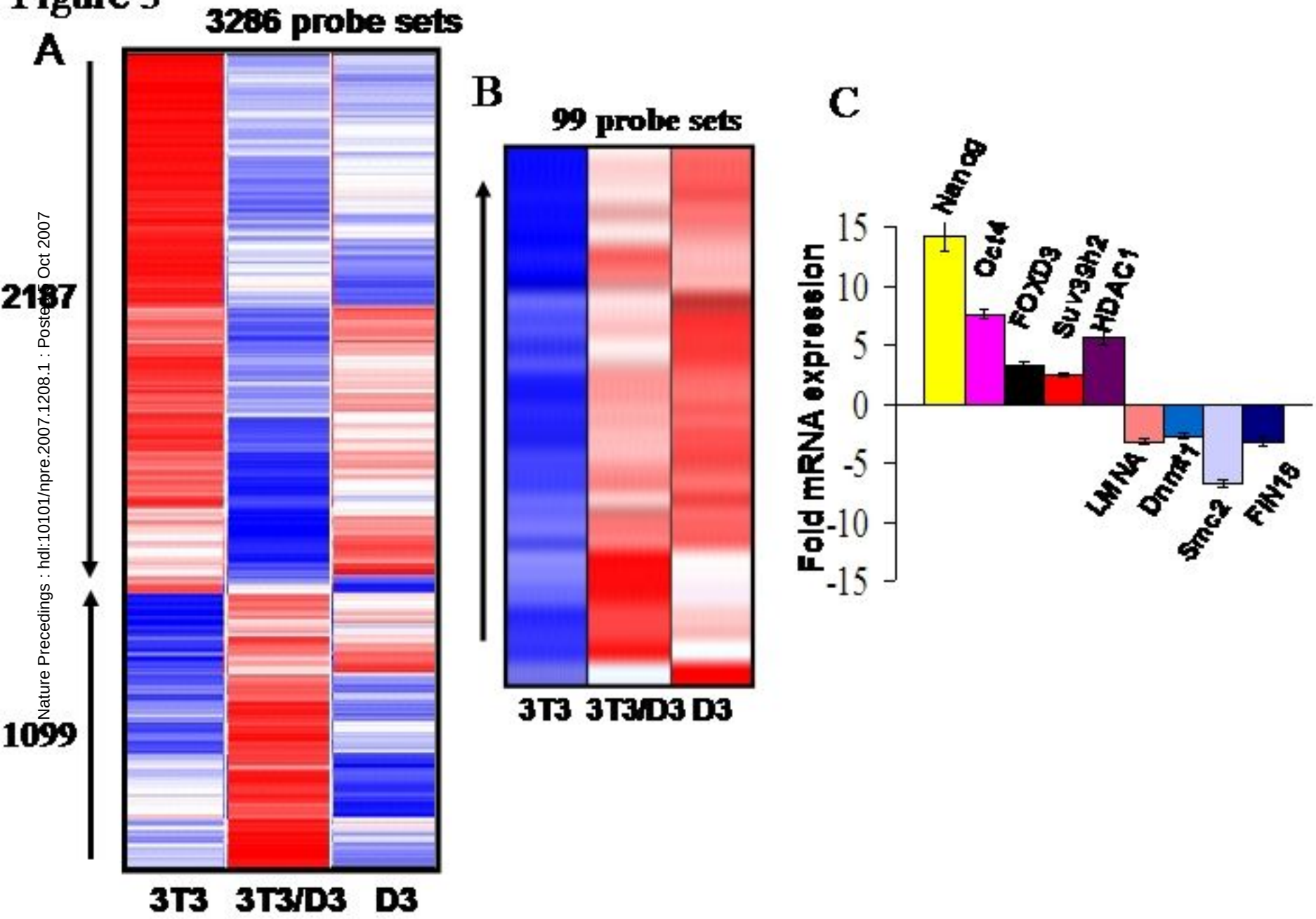

Figure 4

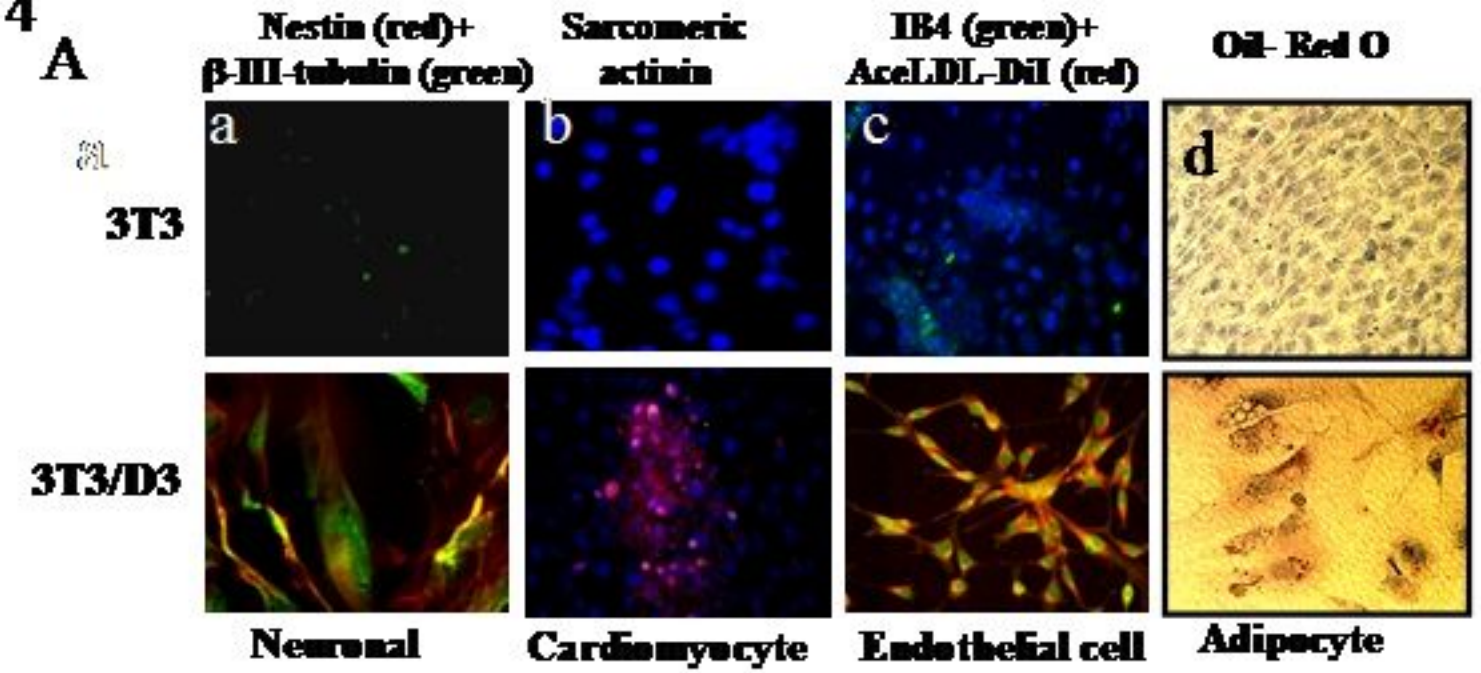

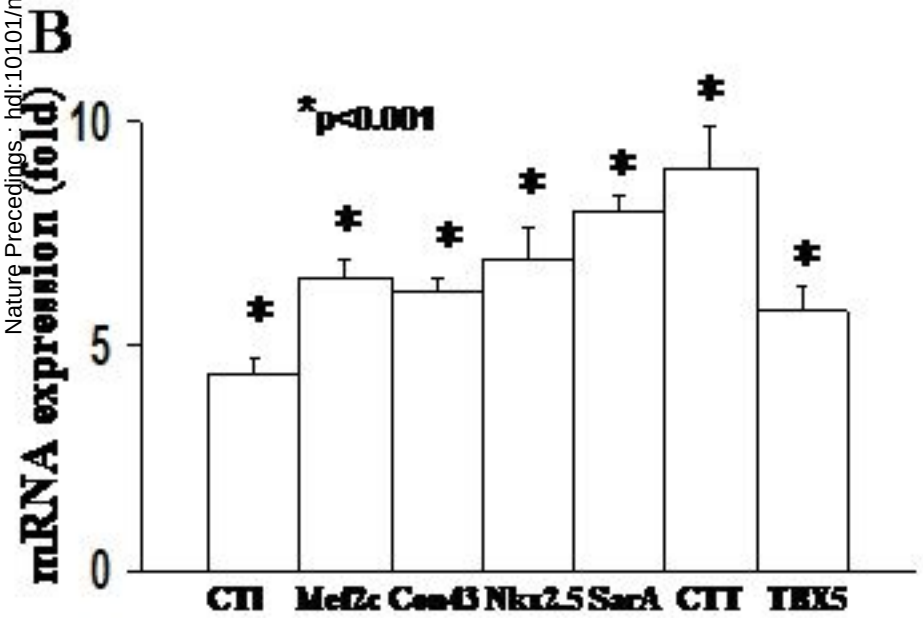

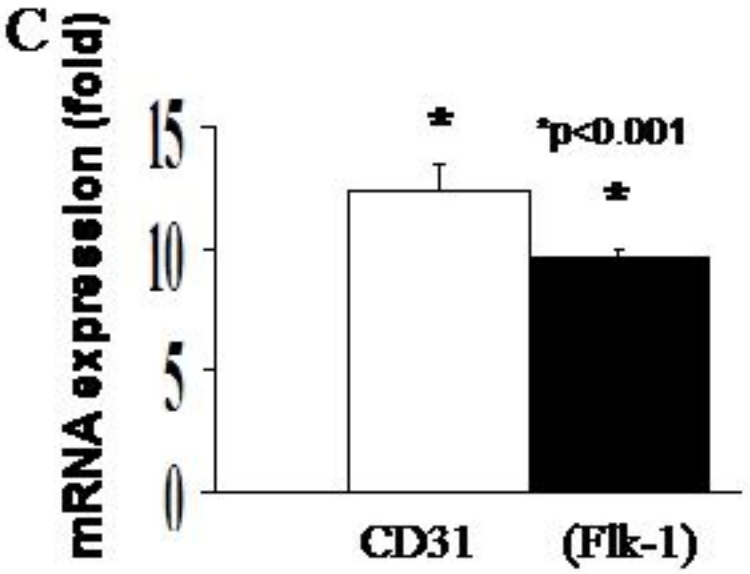

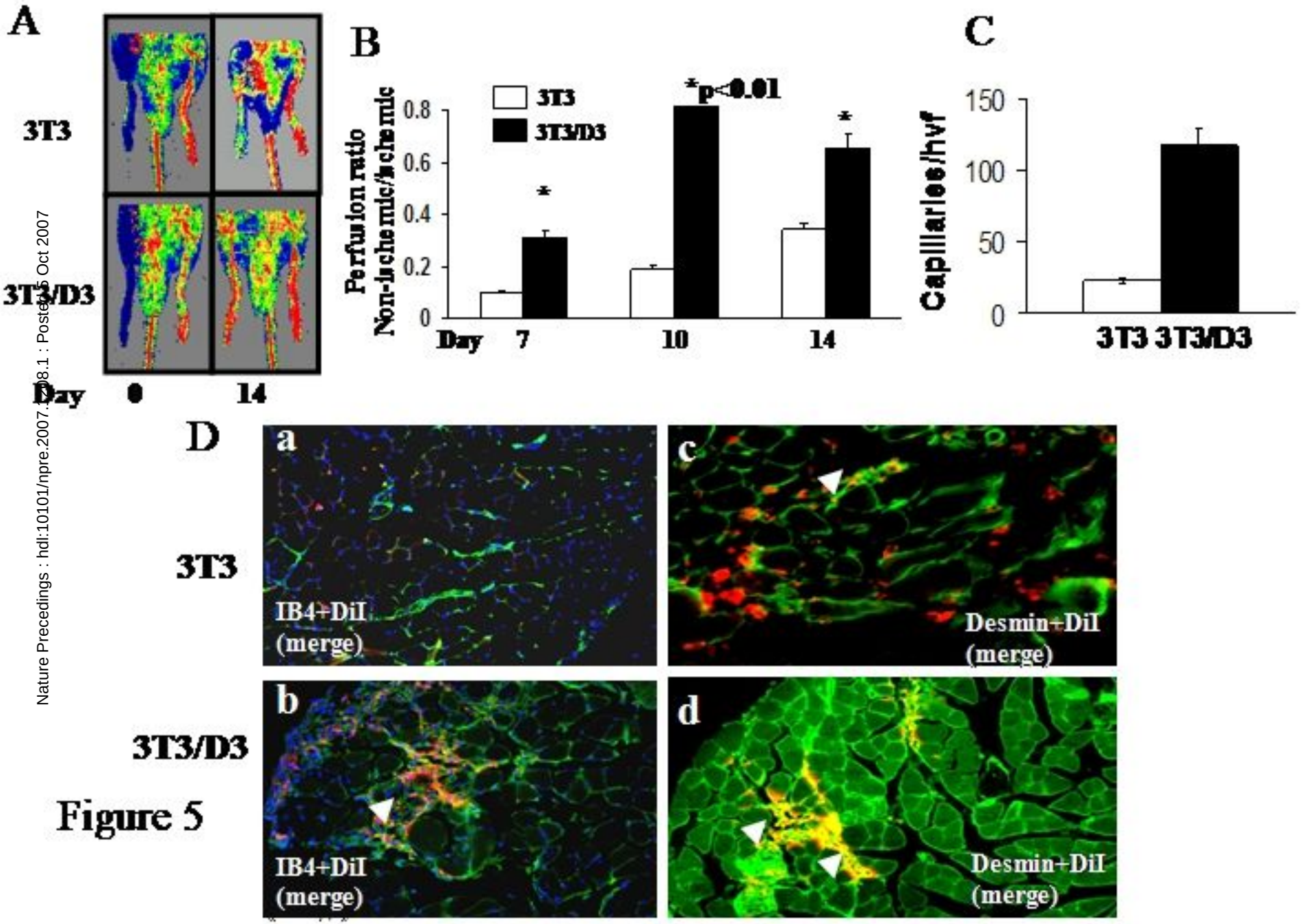

Figure 5

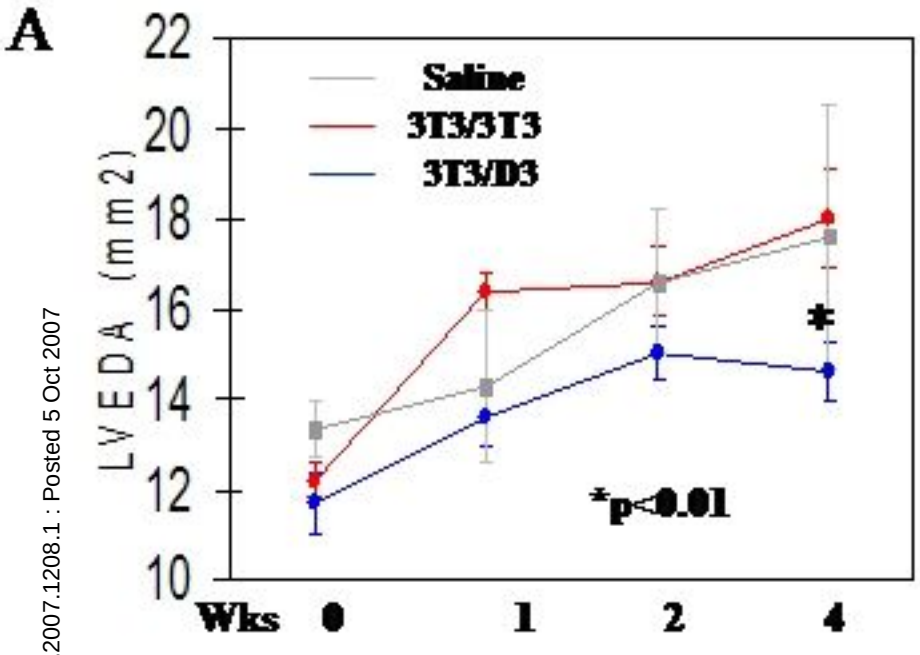

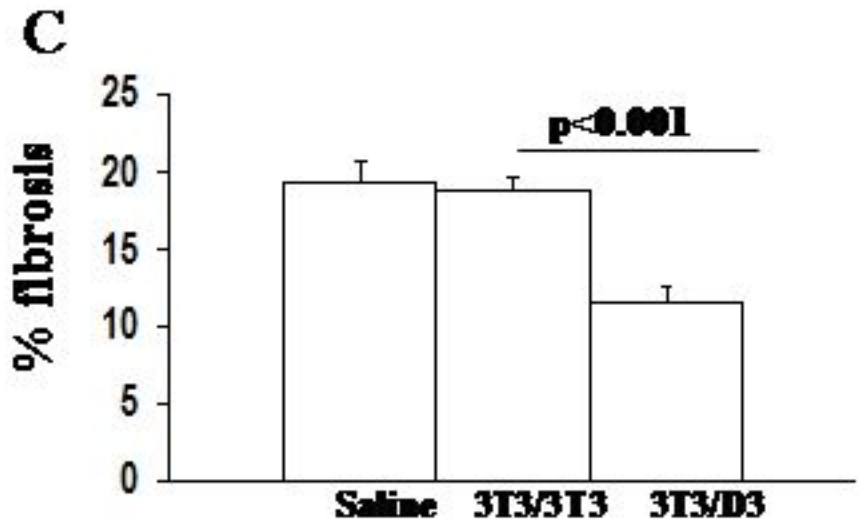

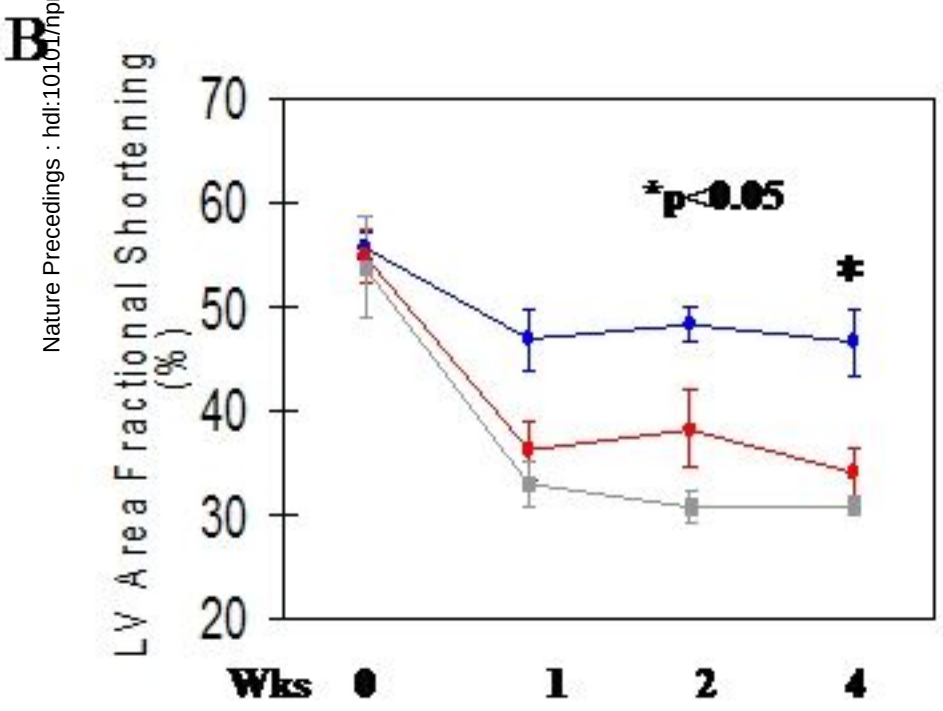

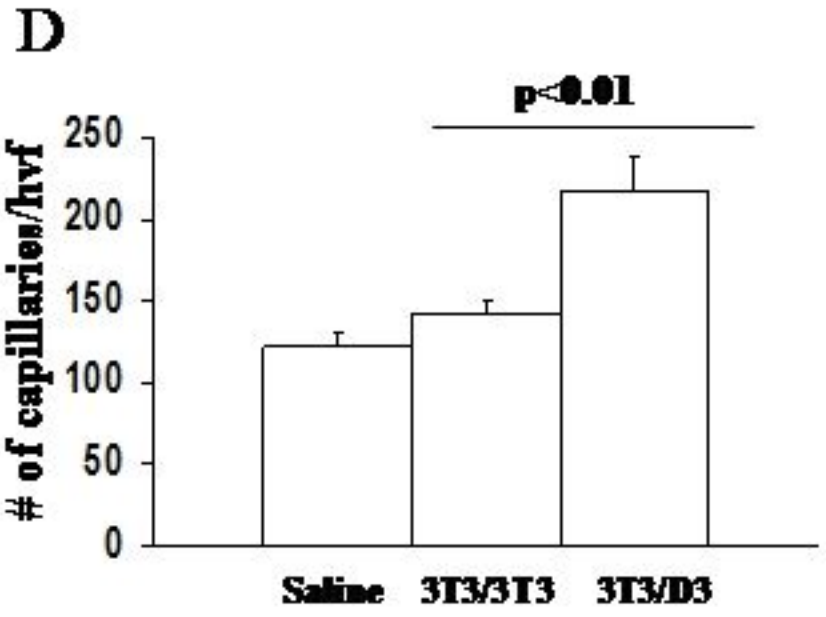

Figure 6

Figure 6E